# THE EFFECT OF A CELL-DEPLETED LAYER NEAR THE WALL ON THE BLOOD FLOW

**Jonas Antonio Albuquerque de Carvalho**
University of Brasilia, Brasilia DF
j0124842@aluno.unb.br

**Francisco Ricardo da Cunha, (corresponding author)**
University of Brasilia, Brasilia DF
frcunha@unb.br

***Abstract.*** *This paper focus on modelling blood flow in micro-vessels by using a generalized Newtonian fluid. We solve the flow problem of two immiscible fluids in vessel of constant cross section. The homogeneous blood is moving in the core of the pipe having a stable interface with a steady small layer of plasma adjacent to the vessel wall. The effect of a variable cross-section capillary on the resistance to the blood flow in microcirculation is also examined. The intrinsic apparent viscosity of the blood and the friction factor of the flow are predicted as a function of the dimensionless vessel diameter and the blood cell volume fraction. In addition we examine how an increase of the plasma viscosity due to an eventual abnormality may affect the apparent viscosity of the flow. The theoretical models suggests that in suspensions flows like blood the apparent viscosity may be much reduced by the no uniform distribution of red cells for vessels. This point is strongly supported by experimental observation of blood flow.*

***Keywords:*** *Cell-depleted layer, Micro circulation, Blood rheology, Blood apparent viscosity.*

## 1. Introduction

In many diseased states, red cell and plasma properties are significantly altered. In sickle cell anaemia, red cells are abnormally rigid, due to changes in the membrane properties and increased internal viscosity. In both sickie-cell anaemia and multiple myeloma, two diseases with quite different causes the resulting pathologies appear to be caused by higher than normal plasma viscosity, an increase tendency to aggregate, and a reduced number of red cells (Schmid-Schönbein, 1981). It has been shown that red cell deformability is reduced in diabetes (Schmid-Schönbein, 1982). Rheological factors are believed to play a role in ischaemia where blood flow to certain peripherical regions is blocked, resulting in pain and tissue damage. Abnormal blood rheology has been associated with many other disease, including malaria and some cancers (Popel & Johnson, 2005).

Blood is a concentrated suspension of red cells, white cells and platelets in plasma. The plasma has approximately the same density $\rho \approx 1000Kg/m^3$ and viscosity $\mu \approx 0.001N\ s/m$ as water. The average volume fraction of red cells (i.e. hematocrit) in the human body is about $40 - 45\%$, although it may vary considerably within the microcirculation. The volume fraction of white cells is less than $1\%$ and platelets occupy an even smaller volume fraction thus, the rheology of blood is primarily determined by red cells (Skalak, Özkay & Skalak, 1989). Red cells must deform considerably to squeeze through capillaries less than $7\mu m$ in diameter. A thin film of plasma separates the cell membrane from the capillary wall. Secomb et al. (1986) exploited the fact that lubrication theory applies in this case, and solved for velocity and shape of a red cell centered in a uniform cylindrical capillary. Membrane area was conserved, and the effects of the induced isotropic tension, shear elasticity, and bending resistance were incorporated. In actuality, red cells are non-axisymmetric, and undergo *tank-treading* as they move through a capillary. Fortunately, and approximative description of non-axisymmetric red cell motion in micro-vessels suggests that tank-treading motion has little rheological effect (Secomb & Hsu, 1996b). The rheological behavior of the blood that arise from the finite size of red blood cells are an essential feature of blood flow in vessels less less than 0.3mm in diameter. The orientation, deformability and shape of the red blood cell has great influences over the rheology of blood in micro-vessels. In low shear rate, the cells assume two concave format and transport the momentum through plasma layers, as the shear grows, the cell gains elongation until all the momentum of the flow is used to preserve this shape, and so on the viscosity decrease as a shear-thinning fluid behavior (Popel & Johnson, 2005).

The cell-depleted plasma layer that forms adjacent to vessel walls is an important example of the behavior of the blood in micro-vessels. The Fahreaus and Fahraeus-Lindqvist effects (Fahraeus, 1929; Fahraeus & Lindqvist, 1931) are the classical manifestations of the cell-depleted layer in micro-vessels. The first describes the reduced hematocrit in vessels less than $0.3mm$ in diameter. Fahraeus (and many subsequent investigators) performed experiments with blood flow in long glass tubes discovering that the tube hematrocit measured by stopping the flow and emptying the tube content was consistently smaller than the discharge hematocrit measured in the discharge reservoir. The second effect describes the concomitant reduction in flow resistance. The apparent viscosity of blood measured in long tubes less than $0.3mm$ in diameter shows a decrease with decreasing diameter, reaching a minimum at diameter of approximately $5 - 7\mu m$, corresponding to the diameter of capillary blood vessels. After this minimum the blood apparent viscosity increases as tube diameter decrease further. This inversion of the Fahraeus-Lindqvist effect corresponds to the regime in which the red blood cells move in single-line flow, one after another (see illustration of this situation in Fig. 1). Significant advances have been made on this flow regime with extensive studies of Skalak and coworkers (Popel & Johnson, 2005).

The existence and physiological significance of the plasma layer in micro-vessels has been empirically established but a fundamental understanding of this phenomenon is unavailable for micro-vessels larger than $7\mu$ in diameter. Approximately 80% of the total pressure drop between the aorta and the vena cava occurs in micro-vessels (Popel & Johnson, 2005). The presence of a cell-depleted

layer near the vessel wall in blood flow that has a significant effect on the pressure drop needed to drive blood flow through the smaller vessels is of vital importance in transport of oxygen-saturated red cells to unsaturated regions. Recent studies of detailed interaction between a red cell and micro-vessel and migration away from the walls that balances hydrodynamic diffusion of the particles induced by shear has been developed to explain the origin of the cell-depleted layer and its influence on resistance to blood flow in microcirculation (Cunha & Loewenberg, 1999; Cunha & Hinch, 1996). According to the review by Skalak, Özkay & Skalak (1989) and more recently by Popel & Johnson (2005), future theoretical research should address the complex behavior of blood flow in micro-vessels that are several red cells wide.

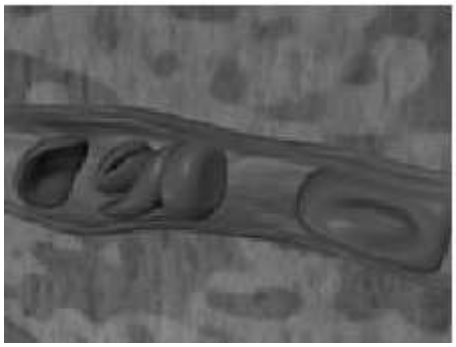

Figure 1. The motion of red-blood cells in a capillary. In this blood flowregime the diameter of the micro-vessel is approximately equal to the red-cell diameter (about $8\mu m$) and consequently the cells move in single-line flow, one after another.

In this paper we present a tentative of modelling the effect of presence of a cell-depleted layer near the vessel wall in blood flow. A two-phase continuum model considering a core of a generalized Newtonian fluid, representing the concentrated blood suspension, and an annual concentric layer of a Newtonian viscous plasma is explored. We have opted to use a Casson fluid model to describe the blood suspension that predicts a yield stress and the well-known shear thinning behavior of the blood. The cell-depleted layer of plasma is simply modelled as a Newtonian fluid. This continuum model has indicated that in suspension flows like blood the apparent viscosity may be much reduced by the non-uniform distribution of red cells in micro-vessels.

## 2. Some Aspects of Red Blood Cell Motion in Micro-vessels

Red blood cells have approximately $90\mu m^3$ volume and $135\mu m^2$ surface area. In the absence of deformation-inducing flow, red cells assume a biconcave disk-shape approximately $8\mu m$ and $2\mu m$, that is, disks with a double-sided dimple at the centre (see illustration in Fig. (2). Red cells suspended in plasma are neutrally buoyant. The cell membrane consists of a mobile double molecular layer of lipids and several proteins which is supported by a rigid network of a protein called spectrin. This rather complex structure renders the red-cell membrane an area preserving (incompressible), two-dimensional medium with small resistance to shearing deformation, and extremely small resistance to bending.

The micro-vessels has diameter over 1mm and lower. Basically, the blood assume three different aspect over this range. For diameters of 0.6 to 1mm the blood still have a homogenous aspect. The red blood cells has uniform distribution and the blood intrinsic viscosity is independent of the vessel diameters size. For healthy person it has a value of 3.0cp (Cunha, 2002). In the range of 0.02 to 0.6mm the red blood cells occupy central region of the blood vessel, and a cell-depleted plasma layer $\delta \approx 2\mu m$ appears. For vessels with diameter up few cell size, the cells travel in single-line (Secomb, 1995). The dynamics is dominated by cell-wall interactions and the rheology of the blood can be accurately predicted by considering the motion of a single red cell. In this regime non-continuum effects of the blood arises from the finite size of the red blood cells and a description of the blood as a homogenous fluid should not be applied.

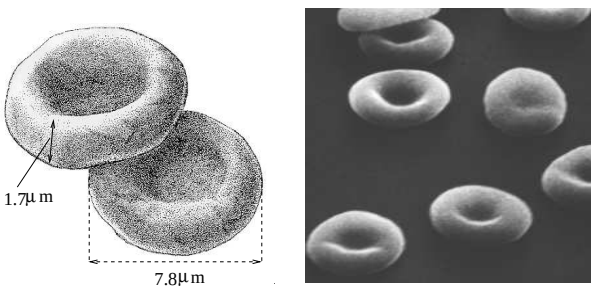


Figure 2. Illustration of a red-blood cell. Red cells are fluid capsules that contain a nearly Newtonian solutions of haemoglobin and are bounded by a flexible biological membrane.

### 2.1 Mechanical properties of red blood cells

Mammalian red blood cells consist of a thin flexible membrane containing the cytoplasm: an aqueous solution of hemoglobin that behaves as a Newtonian fluid with a viscosity several times larger than the plasma, $\mu_i \sim 10^{-2} N\ s/m^2$. The cytoplasm fluid is incompressible; thus, cell volume is preserved. The red cell membrane exhibits viscoelastic properties (Evans & Skalak, 1980) that have been extensively studied ((Popel & Johnson, 2005). According to theses studies, the mechanical properties of the red cell membrane are characterized by four material constants; an elastic modulus of dilatation $E_D \sim 0.5N/m$, an elastic modulus of shear $E_S \sim 6 \times 10^{-6}$, a bending moment $M_B \sim 2 \times 10^{-19} Nm$, and a shear viscosity $\mu_s \sim 10^{-6} N\ s/m$. The large magnitude of $E_D$ indicates that the area of a red cell membrane remains essentially constant. The mammalian red cell is the only biological cell known to have a structureless, liquid interior and an area-preserving membrane. When a red blood cell is placed in a straining flow, it starts deforming much like a liquid droplet. When the straining flow is rotational and the shear rate is above a threshold value, the cell membrane deforms as well as rotates in a *tank-treading* mode, inducing internal circulation (Evans & Skalak, 1980). Unlike a liquid drop, a red blood cell may not deform without limit owing to the virtually constant area of the bounding membrane. As the intensity of the imposed straining flow is increased the membrane tension escalates to higher levels, eventually leading to rupture and haemolysis.

### 2.2 Scaling Arguments

In this subsection some scaling arguments are presented in order to identify the main physical parameter to show that the flow in the microcirculation is characterized by low-Reynolds number flow (Cunha, 2002). Using typical physiological pressure gradient of $\Delta p = 60mm\ Hg$ over $\ell = 1$ centimeter in the microcirculation. The plasma has approximately the same density $\rho \approx 1000 Kg/m^3$ and viscosity $\mu_p \approx 0.001 N\ s/m$ as water. Poiseuille's law for the flow in a micro-vessel of radius $100\mu m$ provides an estimate of the local strain rate $\dot{\gamma} = R\Delta p/(8\mu_p \ell) \sim 10^4 s^{-1}$. On the length scale of a red cell, $a = 5\mu m$, the Reynolds number that characterizes the plasma flow is $Re = \rho \dot{\gamma} a^2/\mu_p \sim 0.1$, confirming that viscous stresses dominate the inertial stresses in the plasma.

Now, using the physical constants that characterize the mechanical properties of red cells, we can form the group of dimensionless parameters shown in Table (1).

Table 1. Dimensionless parameters describing red cell dynamics; typical values for red cell motion in microcirculation.

| **parameter** | **physical significance** | **typical value** |
|---|---|---|
| membrane viscosity ratio: $\lambda_m = \frac{\mu_m}{\mu_p}$ | relative importance of membrane viscosity | $\lambda_m \sim 300$ |
| cytoplasmic viscosity ratio: $\lambda_i = \frac{\mu_i}{\mu_p}$ | relative importance of citoplasmatic flow | $\lambda_i \sim 10$ |
| elastic capillary parameter: $Ca_S = \frac{\mu_p \dot{\gamma} a}{E_S}$ | ratio of viscous stresses to elastic stresses | $C_S \sim 1$ |
| bending parameter: $C_B = \frac{\mu_p \dot{\gamma} a}{M_B}$ | ratio of viscous stresses to bending stresses | $C_B \sim 100$ |
| dilatational parameter: $C_D = \frac{\mu_p \dot{\gamma} a}{E_D}$ | ratio of viscous stresses to dilational stresses | $C_D \sim 10^{-5}$ |
| yield stress parameter: $C_A = \frac{\mu \dot{\gamma}}{\tau_0}$ | ratio of viscous stresses to yield stresses | $C_A \sim 100$ |

The typical parameter values displayed in the table above are obtained from the well-established mechanical properties listed in §(2.1) and the local strain-rate estimate given above.

A number of important conclusions can be drawn on the basis of the dimensionless parameter defined above. The small magnitude of $C_D$ indicates that viscous stress are too small to significantly dilate the red cell membrane; the surface are of a red cell remains essentially constant, as expected. The observations that $\lambda_S \gg \lambda_i$ indicates that membrane viscosity dominates the cytoplasmic viscosity. Thus, the internal circulation of the cytoplasm is largely masked by the membrane viscosity and is expected to have little dynamical effect on red cell motion. This prediction is in agreement with theoretical studies (Barthes-Biesel & Sgaier, 1985; Secomb & Hsu, 1996b). The estimative that $C_S = O(1)$ indicates that the elastic shear stresses are significant, as expected. The bending parameter is large suggesting that bending stress are unimportant. However, bending stresses should be estimated form the curvature radius of the red cell membrane. Thus, we could re-define the parameter $C_B = \mu_p \dot{\gamma}/M_B \kappa^3$, where $\kappa$ is a characteristic curvature. For a deformed red cell, $k$ may be several times larger than $1/a$ thus, $C_B = O(1)$ indicating that stress are important. This finding is in agreement with the predictions of Secomb et al. (1986). The yield stress parameter is large, indicating that in normal condition of the blood yield stress and the tendency for cell aggregates is a small effect. In summary, red cell motion in the micro-vessels is constrained by constant area and is sensitive to three parameters: the membrane viscosity ratio $\lambda_m$, the elastic capillary parameter $Ca_S$, and the bending parameter, $Ca_B$.

## 3. Pressure-driven blood flow in micro-vessels

In this section we consider a continuum model to examine pressure-drive flow of blood in micro-vessels of diameter of order $100\mu m$. We address these studies as being a first starting point to win some insight of the role of the cell-depleted layer on the flow blood resistance and on the apparent viscosity of the blood. The present macroscopic model will suppose the flow of the blood in the micro-vessels corresponding to the flow of two continuum incompressible immiscible fluids; a cell-depleted layer of pure plasma close to the wall and the blood suspension in the core of the vessel. A schematic of the problem is shown in Fig. (3)

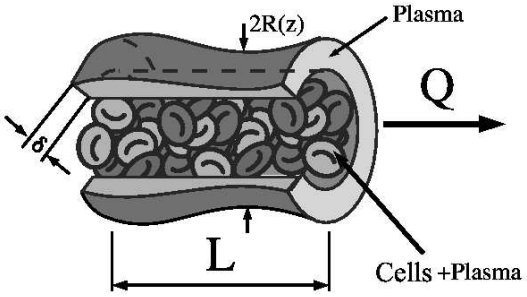


Figure 3. Scheme of the blood flow in micro-vessels of $100\mu m$ describing the geometry of the flow problem studied. The blood suspension travels in the core of the vessel whereas a thin cell-depleted layer containing pure plasma flows adjacent to the wall thickness $\delta$.

### 3.1 Governing equations

The general equations of conservation of mass and momentum for the flow illustrates in Fig. (3) are described next.
For the thin cell-depleted layer containing pure plasma

$$\nabla \cdot \mathbf{u} = 0, \quad -\nabla p + \nabla \cdot \boldsymbol{\tau} = 0. \tag{1}$$

The plasma is considered an incompressible Newtonian fluid of viscosity $\mu_p$, and $\tau = 2\mu_p \mathbf{D}$. Here $\mathbf{u}$ represents the Eulerian velocity field, $p$ is the pressure and $D = (1/2)(\nabla \mathbf{u} + \nabla \mathbf{u}^T)$ denotes the rate of strain tensor of the flow.
For the blood suspension travelling in the core of the vessel

$$\nabla \cdot \mathbf{u} = 0, \quad -\nabla p + \nabla \cdot \boldsymbol{\Sigma} = 0. \tag{2}$$

The blood suspension is modelled as a shear rate dependence viscosity fluid, i.e. $\eta = \eta(\dot{\gamma})$. Therefore the constitutive equation for the blood suspension is expressed as

$$\boldsymbol{\Sigma} = 2\eta(\dot{\gamma})\mathbf{D} \quad , \dot{\gamma} = (2\mathbf{D} : \mathbf{D})^{1/2} \tag{3}$$

An appropriate shear rate dependence apparent viscosity fluid model for describing blood was proposed by Casson (Bird *et al.*, 1987) ad-hoc formula. We have adopted this formula to write

$$\eta(\dot{\gamma}) = \mu_e(\phi) + \frac{1}{2^{1/2}}\tau_0(\mathbf{D} : \mathbf{D})^{-1/2} + \frac{1}{2^{1/4}}C(\mathbf{D} : \mathbf{D})^{-1/4}, \tag{4}$$

where $\mu_e$, $\tau_0$ and $C$ are material constant of the blood and $\phi$ is the volume fraction of the red cells or hematocrit. Here $\mu_e$ denotes a Newtonian viscosity of blood at high shear rate that dependents on the hematocrit, $\tau_o$ is the blood yield stress corresponding to the point in which as increasing the shear stress from zero, the blood first appear to show liquid-like behavior, in that it begins to flow. Human blood in most cases has values of yield stress considerable small. Elevated yield stress values can be found in some pathological situations as elevated rates of lipids and triglycerides and in the case of sickle cell anaemia the tendency of red cells to aggregate or clump together forming small stacks of cells (e.g. Popel and Johnson, 2005). Finally, the material constant $C$ is the shear-thinning constant, wherein $C = 2(\mu_e\tau_0)^{1/2}$ (i.e. a geometric mean). According to this model in the case of $\tau_o = C = 0$ the blood is described as a homogeneous Newtonian fluid with $\boldsymbol{\Sigma} = \mu_E \mathbf{D}$ with a hematocrit dependence viscosity. At moderate shear rate of such as occurs in vessel of diameter of order $0.1mm$ and for small yield stress the behavior of the blood is fully dominated by the shear thinning contribution which dominates the Newtonian part and the yield stress contribution in Equation (4).

### 3.2 The solution of the core axisymmetric blood flow in a tube

We develop in this section the solution for the velocity profile, flow rate, pressure drop and the resulting blood intrinsic apparent viscosity based on our two-phase continuum model. We consider a core of a Casson generalized Newtonian fluid, representing the concentrated red blood cell core suspension in th region $0 \leq r < R - \delta$ and an annual concentric layer of a Newtonian plasma representing the cell-depleted layer in the region $R - \delta \leq r < R$. We suppose that the density of red cells differs only slightly from that of plasma, and buoyancy and gravity effects are neglected here. In this formulation cylindrical coordinates (r,z) are used, the flow

is steady and the pressure in the vessel may depends only on $z$, the axial position. Fig. (3) indicates the geometry and variable of this axisymmetric flow examined. In the present model is also considered the effect of an irregular wall of the micro-vessel on the intrinsic viscosity of the blood. For this end, we have assumed a micro-vessel with sinusoidally varying radius of the form

$$R(z) = R_0 \left[1 + \alpha \sin\left(\frac{2\pi z}{L}\right)\right] \tag{5}$$

where $R_0$ is the mean radius and $\alpha$ denotes the amplitude of the wall disturbance, with $\alpha \ll 1$.

The complete set of governing equations described in §3.1 written in terms of cylindrical coordinates is given by

$$\begin{cases} \dfrac{1}{r}\dfrac{\partial}{\partial r}(r\tau_1) = -\dfrac{\partial p}{\partial z} & 0 \le r < R - \delta \\ \dfrac{1}{r}\dfrac{\partial}{\partial r}(r\tau_2) = -\dfrac{\partial p}{\partial z} & R - \delta \le r < R \end{cases} \tag{6}$$

The subscript 1 and 2 denotes the blood core and the cell-depleted layer, respectively. In addition, according to Fig. (3) the imposed boundary conditions are the non-slip boundary on the vessel wall (no porous vessel), the symmetry condition on the axis of the tube (i.e. no shear stress) and velocity and stress continuity on the interface cells depleted layer-blood suspension. These conditions are expressed mathematically as follows

$$\tau_1(0) = 0; \quad u_1(R(z) - \delta) = u_2(R(z) - \delta); \quad u_2(R(z)) = 0; \quad \tau_1(R(z) - \delta) = \tau_2(R(z) - \delta) \tag{7}$$

Again the subscripts 1 and 2 denotes the blood suspension and plasma fluid respectively, $u$ is the flow velocity, $\tau$ represents the shear stress, $R(z)$ the vessel radius and $\delta$ the thickness of the cell-depleted layer.

Eqs. (6) may be solved by direct integration. Using the boundary condition $\tau_1(0) = 0$ and $\tau_1(R - \delta) = \tau_2(R - \delta)$, respectively, in order to find the integration constant we obtain

$$\begin{cases} \tau_1 = -\dfrac{r}{2}\dfrac{\partial p}{\partial z} & 0 \le r < R - \delta \\ \tau_2 = -\dfrac{r}{2}\dfrac{\partial p}{\partial z} & R - \delta \le r < R \end{cases} \tag{8}$$

Now, expressing the general constitutive description of the blood given by Eqs. (3) and (4) in cylindrical coordinates we have

$$\tau_1 = \left(\sqrt{\tau_0} + \sqrt{\mu_e\left(-\frac{\partial u}{\partial r}\right)}\right)^2 \tag{9}$$

Then, the set of governing equations in terms of the pressure and the axial velocity $u$ is found to be:

$$\begin{cases} \dfrac{\partial u}{\partial r} = -\dfrac{1}{\mu_e}\left[\left(\dfrac{r}{2}\dfrac{\partial p}{\partial z}\right)^{1/2} - \sqrt{\tau_0}\right]^2 & 0 \le r < R - \delta \\ \dfrac{\partial u}{\partial r} = -\dfrac{r}{2\mu_p}\dfrac{\partial p}{\partial z} & R - \delta \le r < R \end{cases} \tag{10}$$

Equations (10) can be solved analytically for the axial velocity in terms of the pressure gradient. So, after integrating over $r$ the result is found to be

$$\begin{cases} u_1 = -\dfrac{1}{\mu_e}\left[\dfrac{r^2}{4}\dfrac{\partial p}{\partial z} - 2^{3/2}\dfrac{r^{3/2}\sqrt{\tau_0}}{3}\left(\dfrac{\partial p}{\partial z}\right)^{1/2} + \tau_0 r\right] + C & 0 \le r < R - \delta \\ u_2 = -\dfrac{\partial p}{\partial z}\dfrac{r^2}{4\mu_p} + D & R - \delta \le r < R \end{cases} \tag{11}$$

Here $C$ and $D$ are integration constants. Applying the non-slip boundary condition in the vessel wall, $u_2(R(z)) = 0$ leads to

$$D = \frac{\partial p}{\partial z}\frac{R^2}{4\mu_p}. \tag{12}$$

By imposing the velocity to be continuous on the blood-cell depleted layer interface, i.e. $u_1(R - \delta) = u_2(R - \delta)$, the value of the constant $C$ must be

$$C = M(z) + \frac{1}{\mu_e}\left[\frac{(R-\delta)^2}{4}\frac{\partial p}{\partial z} - 2^{3/2}\frac{(R-\delta)^{3/2}\sqrt{\tau_0}}{3}\left(\frac{\partial p}{\partial z}\right)^{1/2} + \tau_0(R-\delta)\right] \tag{13}$$

with

$$M(z) = \frac{1}{4\mu_p}\frac{\partial p}{\partial z}\left[R^2 - (R-\delta)^2\right].$$

Now, substituting the values of $C$ and $D$ into Eqs.(11) and also considering explicitly the hard core region of the tube defined by the Bingham radius $R_B = 2L\tau_0/(P_0 - P_L)$ (that corresponds to a rigid body translation motion), the complete axial velocity profile results in the following set of equations

$$u = \begin{cases} \dfrac{R\tau_z}{2\mu_p}\left\{1 + \varsigma^2\left[\dfrac{\tau_0}{\tau_z}\lambda_e^{-1} + \dfrac{\tau_\delta^2}{\tau_z^2}(\lambda_e^{-1} - 1)\right] - \varsigma^{3/2}\left[\dfrac{8\tau_0^2\lambda_e^{-1}}{3\tau_z^2}\left(1 - \dfrac{\tau_\delta^{3/2}}{\tau_z^{3/2}}\right)\right] + \right. \\ \left. \varsigma\left[\dfrac{2\tau_0^2\lambda_e^{-1}}{\tau_z^2}\left(\dfrac{\tau_\delta}{\tau_0} - 1\right)\right]\right\} \text{ for } 0 \le r < R_B \\ \dfrac{R\tau_z}{2\mu_p}\left\{-\lambda_e^{-1}\left(\dfrac{\tau_0}{\tau_z} - \dfrac{r}{2\tau_z}\dfrac{\partial p}{\partial z}\right)^2 - \lambda_e^{-1}\dfrac{8}{3}\dfrac{\sqrt{\tau_0}}{\tau_z^2}\left(\dfrac{\partial p}{\partial z}\right)^{3/2}\left(\dfrac{\sqrt{2}}{4}r^{3/2} - \dfrac{\tau_\delta^{3/2}L^{3/2}}{(P_0 - P_L)^{3/2}}\right)\right. \\ \left. \varsigma^2\dfrac{\tau_\delta^2}{\tau_z^2}(\lambda_e^{-1} - 1) + 2\varsigma\lambda_e^{-1}\dfrac{\tau_0\tau_\delta}{\tau_z^2} + \dfrac{\tau_0^2}{\tau_z^2}\right\} \text{ for } R_B \le r \le (R-\delta) \\ \dfrac{R\tau_z}{2\mu_p}\left(1 - \dfrac{r^2}{R^2}\right) \text{ for } (R-\delta) < r \le R_0 \end{cases} \tag{14}$$

where $\varsigma = \dfrac{-\dfrac{\partial p}{\partial z}L}{(P_0 - P_L)}$; $\tau_z = -\dfrac{R}{2}\dfrac{\partial p}{\partial z}$; $\tau_\delta = \dfrac{(R-\delta)(P_0 - P_L)}{2L}$; $\tau_0 = \dfrac{R_B 2L(P_0 - P_L)}{2L}$; $\lambda_e = \dfrac{\mu_e}{\mu_p}$.

The total volumetric flow rate $Q$ of fluid is calculated by

$$Q = 2\pi\int_0^R urdr = 2\pi\left(\int_0^{R_B} urdr + \int_{R_B}^{R-\delta} urdr + \int_R^{R-\delta} urdr\right), \tag{15}$$

It should be important to note that as a consequence of the cross-section variation the pressure gradient is not constant. In particular, the ratio $\varsigma \neq 1$. For instance, this factor makes difficult a propose of obtaining an analytical expression for the flow rate, $Q$. However, since $\alpha$ is a small parameter (i.e. unidirectional flow) the ratio $\varsigma$ in this limit is pretty close to unit. Under this condition, the pressure gradient given in terms of the flow rate is obtained after performing the integrals of Eq. (15). We found

$$\frac{\partial p}{\partial z} = -\frac{168\, Q\, \lambda_e\, \mu_p}{\pi\left((-21 - 28\,\varepsilon + \varepsilon^4 + 21\,\lambda_e + 48\,\sqrt{\varepsilon})\,(\delta\,\psi - \delta)^4 - 21\,(1+Z)^4\,(\delta 4\,\psi)^4\,\lambda_e\right)}, \tag{16}$$

where $\varepsilon$ denotes the ratio $\tau_0/\tau_\delta = R_B/(R-\delta)$, $\psi = R_0/\delta$ and $Z = \alpha sen(2\pi z/L)$. In order to integrate the pressure gradient along to $z$ direction, equation (16) is re-written in the following form

$$\frac{\partial p}{\partial z} = f(z) = \frac{\mathcal{A}}{\mathcal{B} - \mathcal{C}(1+Z)^4} \tag{17}$$

where $\mathcal{A}$, $\mathcal{B}$, $\mathcal{C}$ are defined as follows

$$\begin{aligned} \mathcal{A} &= -168\, Q\, \mu_e/\pi; \\ \mathcal{B} &= (-21 - 28\,\varepsilon + \varepsilon^4 + 21\,\lambda_e + 48\,\sqrt{\varepsilon})\,(\delta\,\psi - \delta)^4; \\ \mathcal{C} &= 21\delta^4\,\psi^4\,\lambda_e; \end{aligned} \tag{18}$$

Now, since $\alpha$ is a small parameter of the problem, that implies $Z \to 0$, we can make an approximation $O(\alpha^3)$ of the function $f(Z)$ by using the third three terms of the associated Mclaurin series. Thus,

$$f(z) = \frac{\mathcal{A}}{\mathcal{B} - \mathcal{C}} - \frac{4\mathcal{A}\mathcal{C}\alpha\, sen\left(\dfrac{2\pi z}{L}\right)}{(\mathcal{C} - \mathcal{B})(\mathcal{B} - \mathcal{C})} + \frac{\left(\dfrac{16\mathcal{A}\mathcal{C}^2}{(\mathcal{C} - \mathcal{B})^2} - \dfrac{6\mathcal{A}\mathcal{C}}{\mathcal{C} - \mathcal{B}}\right)\alpha^2\, sen\left(\dfrac{2\pi z}{L}\right)^2}{\mathcal{B} - \mathcal{C}} + O(\alpha^3) \tag{19}$$

The pressure drop inside the micro-vessel can be evaluated by

$$\Delta p = \int_0^L f(z)dz \tag{20}$$

Using the software Maple version 8.0 to perform the integral we obtain the following expression for the pressure drop

$$\frac{P_0 - P_L}{L} = \frac{(-2\mathcal{BC} + \mathcal{C}^2 + 5\mathcal{C}^2\alpha^2 + \mathcal{B}^2 + 3\mathcal{C}\alpha^2\mathcal{B})\mathcal{A}}{(\mathcal{B}^2 - 2\mathcal{BC} + \mathcal{C}^2)(\mathcal{C} - \mathcal{B})} \tag{21}$$

Consequently,

$$Q = \frac{-\pi(\mathcal{B}^2 - 2\mathcal{BC} + \mathcal{C}^2)(\mathcal{C} - \mathcal{B})}{(-2\mathcal{BC} + \mathcal{C}^2 + 5\mathcal{C}^2\alpha^2 + \mathcal{B}^2 + 3\mathcal{C}\alpha^2\mathcal{B})168\,\lambda_e\,\mu_p}\left(\frac{P_0 - P_L}{L}\right) \tag{22}$$

Now, the intrinsic apparent viscosity $\mu_s$ of the blood can be determined simple comparing between Eq.22 and the classical Poiseuille Law

$$Q = \frac{\pi R^4(P_0 - P_L)}{8\mu_s L}. \tag{23}$$

The result is

$$\frac{\mu_s}{\mu_p} = \frac{R^4(-2\mathcal{BC} + \mathcal{C}^2 + 5\mathcal{C}^2\alpha^2 + \mathcal{B}^2 + 3\mathcal{C}\alpha^2\mathcal{B})168\,\lambda_e}{8(\mathcal{B}^2 - 2\mathcal{BC} + \mathcal{C}^2)(\mathcal{B} - \mathcal{C})} \tag{24}$$

### 3.3 Blood flow in a micro-vessel of constant cross section

Let us now to consider the particular case of a micro-vessel of constant cross-section, i.e. $\alpha = 0$ and $R = R_0$. Under this condition, the volume flow rate $Q$ evaluated from Eq. (22) reduces to

$$Q = \frac{\pi(R_0 - \delta)^4(P_0 - P_L)}{8\mu_e(\phi)L}G(\varepsilon) + \pi\frac{(P_0 - P_L)R_0^4}{8\mu_p L}\left[1 - \left(\frac{R_0 - \delta}{R_0}\right)^4\right] \tag{25}$$

where the yield stress function $G(\varepsilon)$ of the blood flow is defined as follows

$$G(\varepsilon) = 1 - \frac{16}{7}\varepsilon^{1/2} + \frac{4}{3}\varepsilon - \frac{1}{21}\varepsilon^4 \tag{26}$$

Note that when $\varepsilon = \tau_0/\tau_\delta \to 0$ the yield stress function $G \to 1$. In this case the blood would be treated as an equivalent Newtonian fluid with effective viscosity $\mu_e(\phi)$. Again $\tau_\delta$ is the shear stress acting on $(R_0 - \delta)$ location o the interface, $\mu_p$ is the plasma viscosity, $(P_0 - P_L)$ is the pressure drop along the length $L$ of the micro-vessel length. Equation 25 indicates that an increase in the value of the yield stress $\tau_0/\tau_\delta = R_B/(R_0 - \delta)$ may produce higher resistance to the blood flow in micro-vessels. The consequence would be a strong work done by the heart required to the blood flows in the microcirculation networks. As mentioned before this parameter is commonly associated with the tendency of red-cells to aggregate or clump together.

Again, the intrinsic apparent viscosity $\mu_s$ of the blood is obtained by comparing Eq.25 with the Poiseuille law

$$Q = \frac{\pi R_o^4(P_0 - P_L)}{8\mu_s L}. \tag{27}$$

Therefore,

$$\frac{\mu_s}{\mu_i} = \frac{\frac{\mu_p}{\mu_i}\left(\frac{R_0}{\delta}\right)^4}{\left(\frac{R_0}{\delta}\right)^4 - \left(\frac{R_0}{\delta} - 1\right)^4\left(1 - \frac{\lambda_p}{\lambda_e}G(\varepsilon)\right)} \tag{28}$$

where $\mu_i$ is the viscosity of the internal fluid to the red-cell, that is basically an aqueous solution of hemoglobin, which, under normal conditions, may be considered to be a Newtonian fluid, and $\lambda_p$ is the viscosity ratio plasma-hemoglobin viscosity. The equation written in this form permits us to investigate variations in the apparent viscosity of the blood produce by variation in the plasma viscosity. Plasma viscosity variation occurs due to some blood abnormalities.

## 4. Results

The observed migration at low Reynolds number of red-blood cells away from the wall in micro-vessels and the formation of the cell-depleted layer near the wall result in the mean red-cell velocity being higher than the mean blood velocity (i.e. bulk velocity). Further because the viscosity of the cell-depleted layer is lower than the viscosity of the concentrated red-blood cell core suspension, the apparent viscosity of blood is lower than the bulk viscosity of the uniform suspension as measured in tubes of larger diameter or in Couette viscometers. Fig. 4 shows this effect in terms of the non-dimensional intrinsic apparent viscosity of the blood as a function of the dimensionless micro-vessel radius $R_0/\delta$. It is seen that the continuum model used here is in reasonable quantitative agreement with observation data on apparent viscosity of the blood (Popel & Johnson, 2005) flow in vessel less than $20\mu m$ of diameter. For vessels with diameter below this limit a discrete description would be needed, because our continuum model was not able to capture the

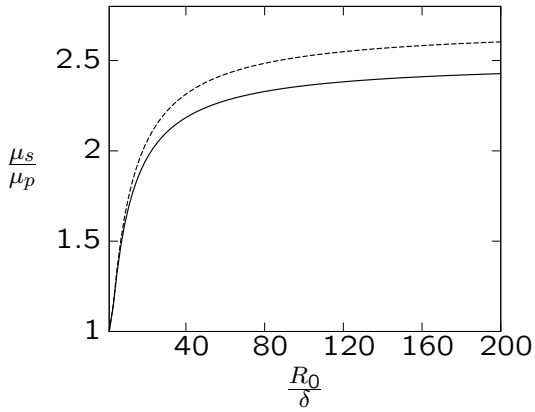


Figure 4. Dimensionless apparent viscosity of the blood as a function of the micro-vessel dimensionless radius $R_o/\delta$. The solid line denotes the Newtonian models and the dashed line the Non-Newtonian model (Casson fluid) for $\alpha = 0$ (no cross-section variation) and $\tau_0/\tau_R = 0.001$.

inversion of the Fahraeus-Lindqvist effect that occurs for flow regime in capillaries where the red-blood cells move in single-file flow. In addition, the plot of Fig. (4) shows a comparison between the apparent viscosity considering the blood core suspension modellated as a Casson fluid and a Newtonian fluid. The Non-Newtonian model is more realistic since it considers the shear thinning behavior of the blood, including the effect of cells to aggregate (yield stress). Owing to these factors the predictions obtained in terms of a shear rate-yield stress dependence viscosity constitutive model of the blood has described better the effect of the cell-depleted layer on the intrinsic viscosity. The Newtonian model under-predicts the blood apparent viscosity and the effect of Fahraeus-Lindqvist is observed for tube radius slightly smaller (i.e. $R_0/\delta < 40$) than those calculated using a non-Newtonian description. When increasing the effect of the yield stress parameter, however, the discrepancy between the two models increases significantly, because the intrinsic viscosity is very sensitive to this parameter. The variation of the apparent intrinsic viscosity, $\mu_s/\mu_i$ over a wide range of the yield stress parameter is shown in Fig. (5). We can see that while the $\mu_s/\mu_i$ is about $1/4$ for very small yield stress parameter (typically as found for a blood in normal physiological condition) an abnormal blood with $\tau_0/\tau_\delta = 1/2$ may present an increase in the intrinsic viscosity about four times. So, depending on the Non-Newtonian properties of the blood under abnormal conditions the values of the intrinsic viscosity are relatively high compared to the Newtonian predictions. The effect of a small disturbance on the vessel wall on the intrinsic blood

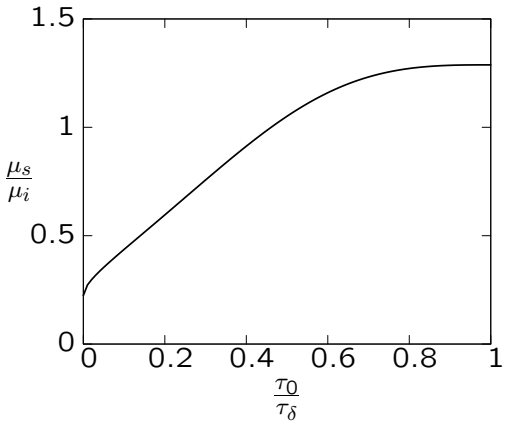


Figure 5. Variations of the dimensionless intrinsic apparent viscosity with yield stress parameter $\tau_0/\tau_\delta$ for $\alpha = 0$ and $R_0/\delta = 100$.

viscosity is presented in Fig. (5). The prediction here indicates that a micro-vessel of non-uniform cross-section with a non-dimensional radius $r_0/\delta \approx 100$ may have an increase in the intrinsic viscosity of approximately $30\%$ for only a small amplitude disturbance in the radius corresponding to $\alpha = 0.005$. This reflects the importance of the wall shape on rheology of the blood flow in the microcirculation since this appears to attenuate the effect of the cell depleted layer producing the observed increase of the blood apparent viscosity. Proceeding, we use the model explored here to examine the effect of variations in the plasma viscosity on the intrinsic blood viscosity. Thus, in Fig. (7) the dimensionless apparent intrinsic viscosity $\mu_s/\mu_i$ as against the dimensionless plasma viscosity $\mu_p/\mu_i$. We see that the variation of the plasma viscosity directly affects the apparent viscosity of the blood in the microcirculation. Consequently diseases and injuries that increase plasma viscosity will promote a high resistance to the blood in micro-vessels. The calculations here suggest that for micro-vessels of $100\mu$, when the plasma viscosity is $\mu_p \approx \mu_i/5$ the apparent viscosity is about $(3/10)\mu_i$. This dependence is more accentuated for plasma viscosity ratio less than $1/5$. Above this limit the model indicate only a slowly variations of the intrinsic viscosity on the plasma viscosity. In fact, the value of plasma viscosity ratio beyond $1/5$ does not make since the viscosity of the

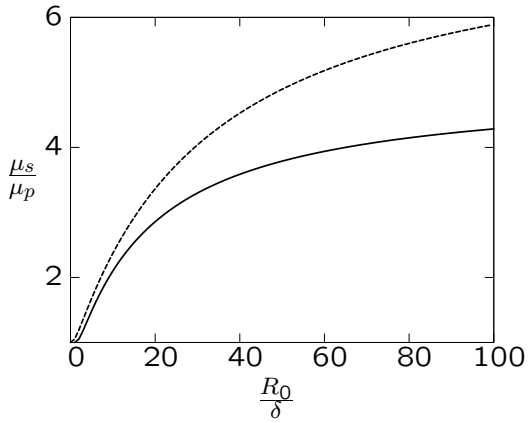


Figure 6. The effect of a cross-section disturbance on the apparent intrinsic viscosity. The solid line denotes $\alpha = 0$ and dashed line $\alpha = 0.005$.

plasma for a healthy blood is about 10 times greater than the plasma viscosity.

In an attempt to reconcile our continuum model with data on the apparent viscosity the model can be also applied to estimate the thickness of the cell-depleted layer $\delta$ Our approaching is also particularly suitable for investigated blood flow under abnormal conditions. The intrinsic viscosity of the blood was shown to depend on the following relevant parameters: the yield stress parameter $\varepsilon = \tau_0/\tau_\delta$ associated with the tendency of cells to aggregate, the cell-depleted layer $\delta/R_0$, the plasma viscosity ratio $\lambda_e$ and the effective viscosity ratio $\lambda_e$ that depends on the hematocrit, $\phi$. As a consequence of diseases such as hypertension, sickle cell anaemia, and diabetes the mentioned parameters may be drastically changed in comparison to the their healthy physiological values, afflicting especially the microcirculation. More recently we have explored the mechanics of cell-cell interactions by a boundary integral method

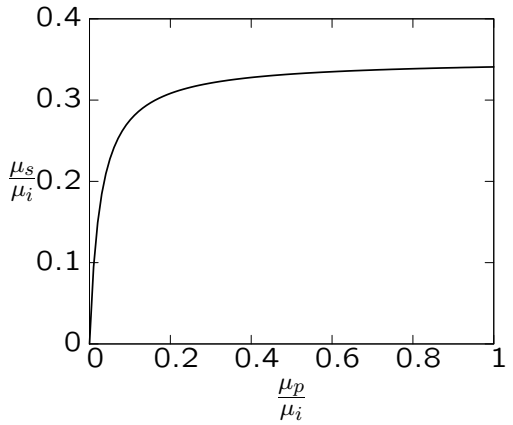


Figure 7. Dimensionless apparent viscosity of the blood as a function of the plasma viscosity ratio $\mu_p/\mu_i$.

(Cunha & Loewenberg, 2003) in order to investigate blood flow accounting the discrete effect of the the red-blood cells and particle migration away from the wall (Cunha & Hinch, 1996). In Fig (8) is shown a preliminary result of our boundary integral simulation with an adaptive mesh on the particle surface for two cells interacting in a periodic suspension. It is seen that the cells deforms during the pair-interaction and this deformation breaks the time reversibility of the particle trajectory leading to a particle a migration across to the streamlines. Based on our previous theoretical studies we have argued that this shear-self-induced migration is they key mechanism responsible to the formation of the cell-depleted layer observed in the microcirculation (Cunha & Hinch, 1996). Moreover, it is interesting to note that the velocity disturbance induced by the motion of the other surrounding particles of the periodic suspension results in cell shapes quite different of the corresponding shapes resulting from a pair of particles interacting in an infinite medium. So, the effect of many-cell-interactions may produce an extra Non-Newtonian contribution to the effective blood suspension directly related to the more complex shape of the cells.

## 5. Closing remarks

The model presented in this article has been very successful in predicting apparent viscosity as a function of the vessel size and the effect of a variable cross-section. The overall aim of the studies reported here has been to understand the intrinsic apparent viscosity of the blood in terms of a continuum description of the blood as a Newtonian generalized fluid with yield stress and shear thinning effects. These findings were in qualitative agreement with experimental observations. Our scaling arguments has suggests that the

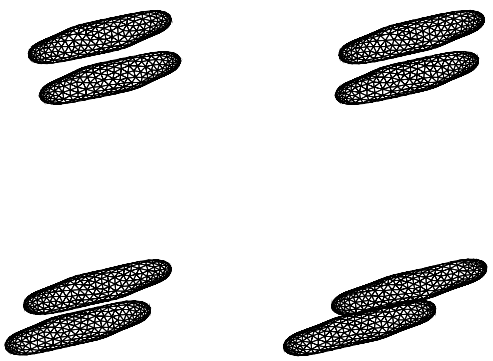

Figure 8. Results of boundary integral simulation of an adaptive mesh on the on particle surface. The suspension is simulated as being a periodic system (i.e. having periodic boundary conditions). The figure shows a sequence of two prototypical cells interacting in a simple shear flow at low Reynolds number. The cells were initially spherical. Details of the numerical simulations are given in (Cunha & Loewenberg, 2003).

effect of a membrane viscosity on the motion of a red blood cell should dominates the dynamical influence of internal circulation of the cytoplasm. The calculations and models presented here may be useful in the future to help understanding the connection between flow resistance or even vessel blockage with blood abnormalities. The theoretical models suggests that in suspensions flows like blood the apparent viscosity may be much reduced by the no uniform distribution of red cells for vessel with diameter up few cell size. This point is strongly supported by experimental observation of blood flow. However, much work is required to understand non-symmetric and complex multi-cells interactions in micro-vessels with diameter order of $100\mu m$.

## 6. Acknowledgements

The authors acknowledges the financial support of CNPq-Brazil and Finatec-UnB.

## 7. References

Barthes-Biesel, D. & Sgaier, H. (1985) Role of membrane viscosity in the orientation and deformation of a spherical capsule suspended in shear flow. *J. Fluid Mech.* **160**, 119.

Bird, R. B., Armstrong, R. C., Hassaer, O., 1987, *Dynamic of polymeric liquids*, vol. 1, Wiley.

Cunha, F.R., & Hinch, E.J., 1996, "Shear-induced dispersion in a dilute suspension of rough spheres", *J. Fluid Mech.*, **309**, 211.

Cunha, F.R., 2002, "Caracterization of capsules and drops motion in micro-vessels for developing of models of the blood flow in the microcirculation", *CNPQ-Report-520386*, **1**, 45p.

Cunha, F.R., & Loewenberg M., 2003, "A study of emulsion expansion by a boundary integral method". *Mechanics Research Comm.*, Vol. **30/6**, 639.

Cunha, F.R., & Loewenberg Michael, 1999. Distribution of deformable particle in shear flow adjacent to a rigid wall. *Proceedings of Biomedical Engineering Research Conference* **1** 119.

Evans, E.A. & Skalak, R. (1980) *Mechanics and Thermodynamics of Biomembranes*, CRC, Boca Raton, Florida.

Fahraeus, R. (1929) The suspension stability of blood. *Physiol. Rev.* **9**, 241.

Fahraeus, R. & Lindqvist, T. (1931) The viscosity of blood in narrow capillary tubes. *Am. J. Physiol.* **96**, 562.

Popel, A.S., Johnson, P.C. (2005) Microcirculation and Hemorheology. *Ann. Rev. Fluid Mech.* **37**, 43.

Schmid-Schönbein, H. (1981) Factors promoting and preventing the fluidity of blood, 249–266, In: *Microcirculation: Current Physiologic, Medical, and Surgical Concepts*, Eds. Effros, RM et al., Academic Press.

Schmid-Schönbein, H. (1982) Normal and pathological distribution of blood flow in the microcirculation, 281–299, In: *Microvascular and ischemic vascular diseases: clinical and therapeutic approaches*, Proceedings of Congress- Rio de Janeiro.

Secomb, T.W., Skalak, R., Özkaya, N. & Gross, J.F. (1986) Flow of axisymmetric red blood cells in narrow capillaries. *J. Fluid Mech.* **163**, 405.

Secomb, T.W. (1995) Mechanics of blood flow in the microcirculation, 305–321, In : *Biological Fluid Dynamics*, Eds. C.P. Ellinton & T.J. Pedley, Company of Biologists, Cambridge.

Secomb, T.W. & Hsu, R. (1996b) Analysis of red blood cell motion through cylindrical micropores: effects of cell properties. *Biophys. J.* **71**, 1095.

Skalak, R., Özkaya, N. & Skalak, T.C. (1989) Biofluid mechanics. *Ann. Rev. Fluid Mech.* **21**, 167.